Advantages and Limitations of Hydrogen Peroxide for Direct Oxidation of Methane to Methanol at Mono-Copper Active Sites in Cu-Exchanged Zeolites

Lu Cheng[a], Xuning Chen[a], P. Hu[a, b], Xiao-Ming Cao [a, *]

[a] *Joint International Research Laboratory for Precision Chemistry and Molecular Engineering, Centre for Computational Chemistry and Research Institute of Industrial Catalysis, School of Chemistry and Molecular Engineering, East China University of Science and Technology, Shanghai 200237, China*

[b] *School of Chemistry and Chemical Engineering, The Queen's University of Belfast, Belfast BT9 5AG, United Kingdom*

* Xiao-Ming Cao.
E-mail address: xmcao@ecust.edu.cn

Abstract： The oxidant is a crucial factor affecting the performance of direct oxidation of methane to methanol (DMTM). It is still extremely challenging to realize one-pot DMTM using dioxygen. So far, hydrogen peroxide is still the most frequently reported green oxidant for DMTM with high selectivity of methanol. Aiming to achieve insights into the influence of oxidants on the DMTM performance and to improve catalysts, we computationally investigated the reaction mechanisms of DMTM using hydrogen peroxide at mono-copper sites in three kinds of Cu-exchanged zeolites with different sizes of the micropores. We identified the common advantage and limitations of hydrogen peroxide as the oxidant. In contrast to dioxygen, the O-O bond of hydrogen peroxide could be easily broken to produce reactive surface oxygen species, enabling the facile C-H bond activation of methane at a lower temperature. However, the radical-like mechanism for the C-H bond activation in DMTM using hydrogen peroxide makes the C-H bond breaking of methanol ineluctably superior to methane. This leads to the inevitable trade-off between selectivity and activity for DMTM. Moreover, the lower O-H bonding energy of hydrogen peroxide would also result in the significant self-decomposition of hydrogen peroxide. Despite the existence of these bottlenecks, the kinetic analysis manifests that it is still promising to improve catalysts to boost the performance of DMTM using hydrogen peroxide.

Keywords: Density Functional Theory, Cu-Exchanged Zeolites, Hydrogen Peroxide, Methane Partial Oxidation, Methanol

1. Introduction

As the most rapidly growing fossil fuel to 2035[1], natural gas plays an increasingly important role in energy generation and chemicals manufacture.[2-4] Considering its high transportation cost, it is always desirable to upgrade its main component, methane (CH_4), to liquid fuels such as methanol (CH_3OH). Ideally, the direct catalytic oxidation of methane to methanol (DMTM) could realize CH_4 upgrading, which is a green chemistry reaction and thermodynamically favorable at ambient temperature. However, it is incredibly challenging because of the low affinity for electrons and protons, the low polarizability, the strongest C-H bond among alkanes (439 $kJ\cdot mol^{-1}$), and the high ionization energy of CH_4.[5] Although many materials can catalyze methane activation and oxidation, the weaker C-H bonds of produced oxygenates readily lead to the deep oxidation and the production of a large amount of carbon dioxide (CO_2).[6-9] It is almost formidable to achieve high activity and selectivity simultaneously for CH_4 partial oxidation , although the researchers have studied DMTM in modern science for decades.[10-17] Nevertheless, interestingly, DMTM could efficiently occur in nature with the help of soluble or particulate methane monooxygenases (MMO) under aerobic conditions at room temperature.[18]

Inspired by pMMO with copper sites which can activate methane by decomposing molecular oxygen,[19-22] the pMMO-like catalysts such as the molecular sieve with copper are regarded as one kind of promising DMTM catalysts.[23-28] Leshkov and colleagues reported the first demonstration of DMTM using molecular oxygen (O_2) on the copper-exchanged zeolite.[29] However, the reaction has to consist of two alternated steps: (1) O_2 activation at a high temperature and (2) CH_4 oxidation at a low temperature.[30-33] Recently, Li and colleagues showed that a high selectivity of 91% CH_3OH over Cu-CHA with a yield of 543 mmol/mol$_{Cu}$/h at 573 K could be achieved using O_2 with the assistance of water.[34] Still, the activity and selectivity of one-pot DMTM reaction using O_2 are limited at a low temperature by the trade-off between C-H bond activation and deep oxidation of CH_3OH.

Identifying the active center of copper zeolite is of prime significance for improving catalysts. Despite numerous characterization methods to clarify the structure of the active site, [27, 30, 35-37] it remains in debate. Many characterization data have indicated that the binuclear copper center is an effective active site in the two-step reaction.[38, 39] Bokhoven and his co-workers proposed that high methanol yields require highly dispersed copper oxide species.[40] They further showed that mononuclear copper was the active center for DMTM in Cu-MOR as confirmed by *in situ* NMR and IR spectroscopy.[41, 42] Kulkarni et al. computationally identified the mononuclear $[Cu^{II}OH]^+$ as the active center of copper-exchanged SSZ-13 for methane partial oxidation reaction.[43] Yashnik et al. suggested that the isolated mononuclear Cu site in Cu-ZSM-5 is one of the possible active sites for DMTM.[44, 45] In particular, Meyet et al. found that synthesized monomeric copper sites could selectively convert methane to methanol and obtain good catalytic activity as well.[46] Mono-copper is possible to be the active site for DMTM.

The oxidant is also a crucial factor governing the performance of DMTM. In contrast to O_2, another green oxidant, hydrogen peroxide (H_2O_2), can more efficiently upgrade CH_4 with high selectivity toward CH_3OH simultaneously at a lower temperature. Fan's group found that the high H_2O_2 utilization could promote the DMTM at a low temperature.[47] Hutchings and his colleagues found that copper addition in Cu-ZSM-5 can provide up to 97 % CH_3OH selectivity in the presence of H_2O_2 at 50°C.[48] Tang et al. reported that Cu_1-O_4/ZSM-5 single atom catalyst exhibits a 99% selectivity of C1 oxide with high conversion of CH_4 at 50 °C.[49] However, H_2O_2 is likely to readily generate the free radicals of ·OH and ·OOH as well, thereby possibly triggering a Fenton reaction and reducing the CH_3OH selectivity.[14, 50, 51]

Inspired by previous work, we were dedicated to computationally investigating the features of H_2O_2 as an oxidant for DMTM at mono-copper sites in Cu-exchanged zeolites to provide the guidelines for improving the catalysts and optimizing reaction conditions.

First, we computationally explored the most stable mononuclear-copper species at Cu-ZSM-5, Cu-MOR, and Cu-SSZ-13. Then, the performances for the activations of O-O bond and methane were computationally compared between O_2 and H_2O_2 as oxidants under the reaction conditions. And, we further studied the complete catalytic cycle from CH_4 to CH_3OH and competitive reaction pathways. Finally, the competition among CH_4, CH_3OH, and H_2O_2 oxidation was discussed in detail upon both energetic and kinetic analysis to understand the limitation of using H_2O_2 as the oxidizing agent.

2. Methods

2.1 Computational Details

The periodic density functional theory (DFT) calculations were applied using Vienna Ab-initio Simulation Package (VASP)[52, 53] in simulating the heterogeneous reactions in the zeolite.[54, 55] The electronic exchange-correlation energy was processed by the Perdew, Burke, and Ernzerhof (PBE) functional in the framework of generalized gradient approximation (GGA).[56] The van der Waals interaction in the zeolite systems was described by the semi-empirical DFT-D3(BJ) method.[57, 58] The plane-wave basis set was employed with a cutoff energy of 400 eV. The geometry optimization of intermediates was performed based on the conjugate gradient method, while the transition state was searched using the constrained optimization method based on the L-BFGS algorithm[59]. The convergence criteria were set as 0.05 eV/Å for the maximal force of all the relaxed atoms. For the gaseous reaction, all the calculations were carried out using Gaussian 09 [60] at the level of M06-2X/aug-cc-pvTZ.

The free energy was calculated with the total energy from DFT calculations corrected by statistical mechanics based on Boltzmann distribution under the reaction condition, including the influence from the zero-point energy, internal energy variation, and entropy.[61, 62] For the free gaseous molecules, the ideal gas model was adopted. The standard free energy of the solute (1M) in the aqueous solution was calculated with its standard gaseous free energy (1 bar) corrected by its solvation energy and the chemical potential variation corresponding to the unit change from 1 bar to 1M. The SMD model was employed to simulate the solvation energy.[63, 64] The chemical potential of the liquid state was calculated based on the phase equilibrium between gas phase and liquid state:

$$\mu_l = \mu_g = G_g^o + RTln(P/P^o) \quad (1)$$

where P is the saturated pressure of the molecule at the reaction temperature.

For the chemisorbed adsorbates, only the vibrational contribution was considered. Due to the restricted translation and rotation of the gaseous molecules in the micropores of zeolites, the lost translational and rotational entropies in different zeolites were corrected following the values from Dauenhauer et al.'s work,[65] which was verified by Mikkel et al.. [66]

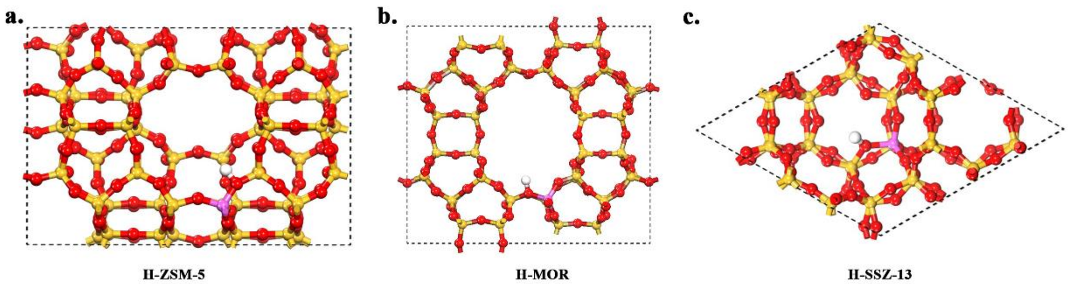

Figure 1. The optimized structure of **(a)** H-ZSM-5 with the unit cell of 20.517 Å × 20.293 Å × 13.627 Å, **(b)** H-MOR with the unit cell of 18.279 Å × 20.463 Å × 7.546 Å, and **(c)** H-SSZ-13 with the unit cell of 13.686 Å × 13.686 Å × 14.771 Å from the view of Z axis. The most stable substituted single Al cations are respectively located on the γ-8MR at the intersection of the straight channel and the sine channel of ZSM-5 zeolite, the 6MR of SSZ-13 zeolite, the 12MR of the straight channel of MOR zeolite. The H, C, O, Si, Al and Cu atoms are displayed in white, gray, red, yellow, magenta, and orange, respectively. This setting would be used throughout the paper.

The DFT simulations for the ZSM-5, MOR, and SSZ-13 used 1×1×1(Γ-point), 1×1×2, and 2×2×2 k-point integration of the Brillouin zone, respectively. The used periodic slab of H-ZSM-5, H-MOR, and H-SSZ-13 are displayed in **Figure 1**. The optimized lattice parameters are consistent with previous experimental data.[67-69] Since a high Si/Al ratio is conducive to improving the yield and selectivity of methanol,[70, 71] the model with single Al substitution was utilized. The energetically most stable site for the single Al substitution was adopted as the active site where the copper species would be anchored. The results are consistent with the previous studies. [72-75]

2.2 *Ab initio* thermodynamic analysis

The stabilities of mono-copper species in the zeolites were studied using *ab initio* thermodynamic analysis. According to the general preparation process, the different copper species ($\mathrm{Z[Cu}_x\mathrm{O}_y\mathrm{H}_z]$) are produced from the copper(II) cations in the aqueous solution, H-zeolite ($\mathrm{Z[H_Z]}$), gaseous O_2, and water:

$$x\mathrm{Cu}^{2+}(\mathrm{aq}) + \mathrm{Z[H}_z] + \frac{2y-z+1}{4}\mathrm{O}_2 + \frac{z-1}{2}\mathrm{H}_2\mathrm{O} \rightleftharpoons \mathrm{Z[Cu}_x\mathrm{O}_y\mathrm{H}_z] \quad (2)$$

Hence, the stabilities of copper species would be evaluated according to the corresponding Gibbs free energy variation as follows:

$$\Delta G(T,p) = G_{\mathrm{Z[Cu}_x\mathrm{O}_y\mathrm{H}_z]} - xG_{\mathrm{Cu}^{2+}(aq)} - G_{\mathrm{Z[H}_z]} - \frac{2y-z+1}{4}\mu_{\mathrm{O}_2} - \frac{z-1}{2}\mu_{\mathrm{H}_2\mathrm{O}} \quad (3)$$

where the Gibbs free energy of Cu^{2+}(aq), $G_{\mathrm{Cu}^{2+}(aq)}$, was calculated according to the Gibbs free energy of bulk Cu from DFT calculations with the correction by the difference of the formation free energies between bulk Cu and Cu^{2+}(aq) from the CRC Handbook of Chemistry and Physics,[76] namely,

$$G_{\mathrm{Cu}^{2+}(aq)} = G_{\mathrm{Cu-bulk}} + (\Delta_f G^o_{\mathrm{Cu}^{2+}(\mathrm{aq})} - \Delta_f G^o_{\mathrm{Cu(s)}}) \quad (4)$$

3. Results and discussions

3.1 Structure, stability and electronic properties of mono-copper species

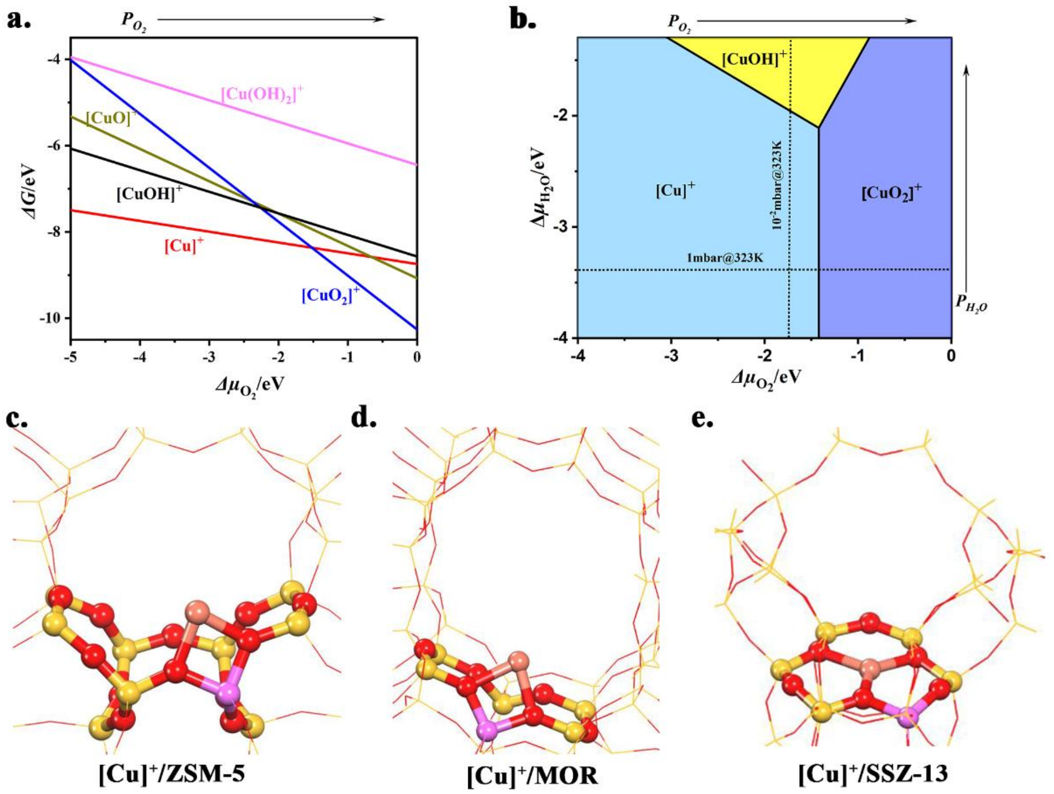

Figure 2. (a) The Gibbs free energies of different mononuclear copper species against $\Delta\mu_{O_2}$ at the reaction temperature of 323 K; **(b)** the phase diagram of Z[$Cu_xO_yH_z$] before the catalysis, at which the dotted line is the most stable copper species before DMTM at 323 K, and the optimized structure of the most stable mono-copper species at 323 K of **(c)** $[Cu]^+$/ZSM-5, **(d)** $[Cu]^+$/MOR, **(e)** $[Cu]^+$/SSZ-13.

We computationally simulated the stabilities of mono-copper species under different conditions. Taking Cu-ZSM-5 as an example, it is clear from **Figure 2a** that Z$[Cu]^+$and Z$[CuO_2]^+$ would be sequentially the most stable species at the fixed chemical potential of water as the partial pressure of O_2 increases at the reaction temperature of 323 K. On the contrary, $Z[CuO]^+$, $Z[CuOH]^+$, and $Z[Cu(OH)_2]^+$ are less stable, which could be owing to the formation of less stable Cu^{3+} or $\cdot O^-/\cdot OH$ to match the valence of $Z[CuO]^+$, $Z[CuOH]^+$ and $Z[Cu(OH)_2]^+$. As displayed in **Figure 2b**, $Z[Cu]^+$ is the most stable mononuclear species for Cu-ZSM-5 before DMTM at 323 K. Likewise, $Z[Cu]^+$ is also the most stable mononuclear copper species for Cu-MOR and Cu-SSZ-13 before DMTM (**Figure S1**).

3.2 Reaction mechanisms of methane partial oxidation towards methanol

3.2.1 O-O bond activation

Notably, H_2O_2/O_2 would preferentially occupy $Z[Cu]^+$ due to the weak adsorption of methane, as evidenced by **Figure 3a**. Accordingly, the methane oxidation would be triggered by O-O bond activation first. We still take Cu-ZSM-5 as the example to elucidate the mechanism for the O-O activation of H_2O_2 at $Z[Cu]^+$ site. As displayed in **Figure 4a**, the H_2O_2 would chemisorb atop $Z[Cu]^+$ via monodentate adsorption mode with the free energy of adsorption of -0.37 eV (IM1). Its O-O bond could be directly scissored to generate $Z[Cu(OH)_2]^+$ after climbing over a free energy barrier of 0.63 eV, releasing the free energy of 1.04 eV. The free energy barriers of this step are similar in Cu-MOR and Cu-SSZ-13. Hence, the O-O bond activation of H_2O_2 is easy in mononuclear copper zeolites. Intriguingly, water could make this process pretty easy. At the TS of O-O bond breaking (TS2), one H_2O molecule could provide a hydrogen atom to assist the O-O bond breaking of H_2O_2. The O-H bond at H_2O and the O-O bond in H_2O_2 are respectively elongated to 1.225 Å and 2.246 Å at TS2. Hence, two OH* (the asterisk denotes the species adsorbed at Cu site) at $Z[Cu(OH)_2]^+$ respectively come from H_2O and H_2O_2 molecules, while the other OH from H_2O_2 regenerates H_2O. This water-mediated process lowers the free energy barrier of O-O activation to only 0.16 eV. Likewise, the DFT calculation results (**Figure S5** and **Figure S6**) show that water-mediated process could readily activate the O-O bond of H_2O_2 to generate $Z[Cu(OH)_2]^+$ in Cu-MOR and Cu-SSZ-13 as well. Hence, the O-O bond activation of H_2O_2 is almost effortless at mono-copper sites and is not very sensitive to the pore sizes of zeolites.

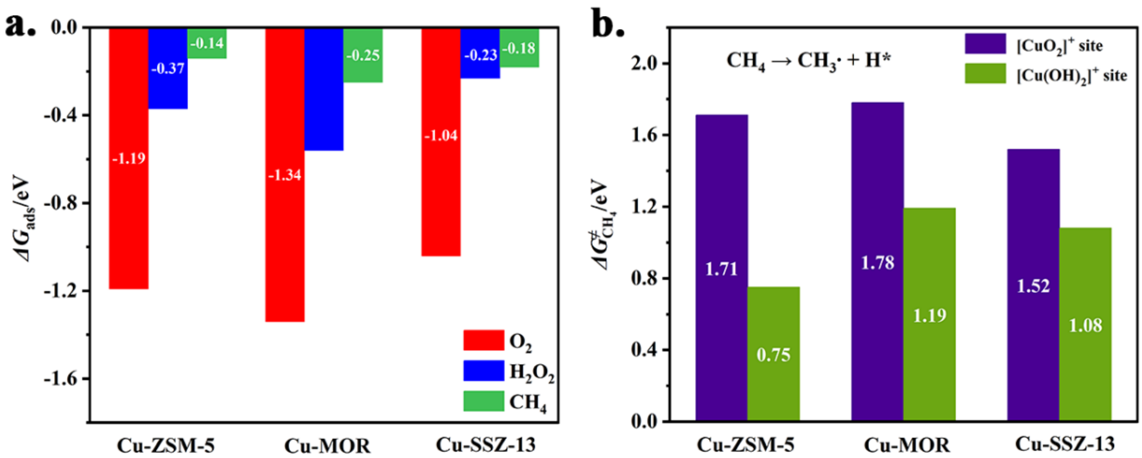

Figure 3. (a) The standard free energies of adsorption for O_2 and H_2O_2 at $Z[Cu]^+$ site in the copper-exchanged zeolites, and **(b)** the standard free energies of activation for the first C-H bond breaking of CH_4 at $[CuO_2]^+$ and $[Cu(OH)_2]^+$ sites in the copper-exchanged zeolites at 323 K.

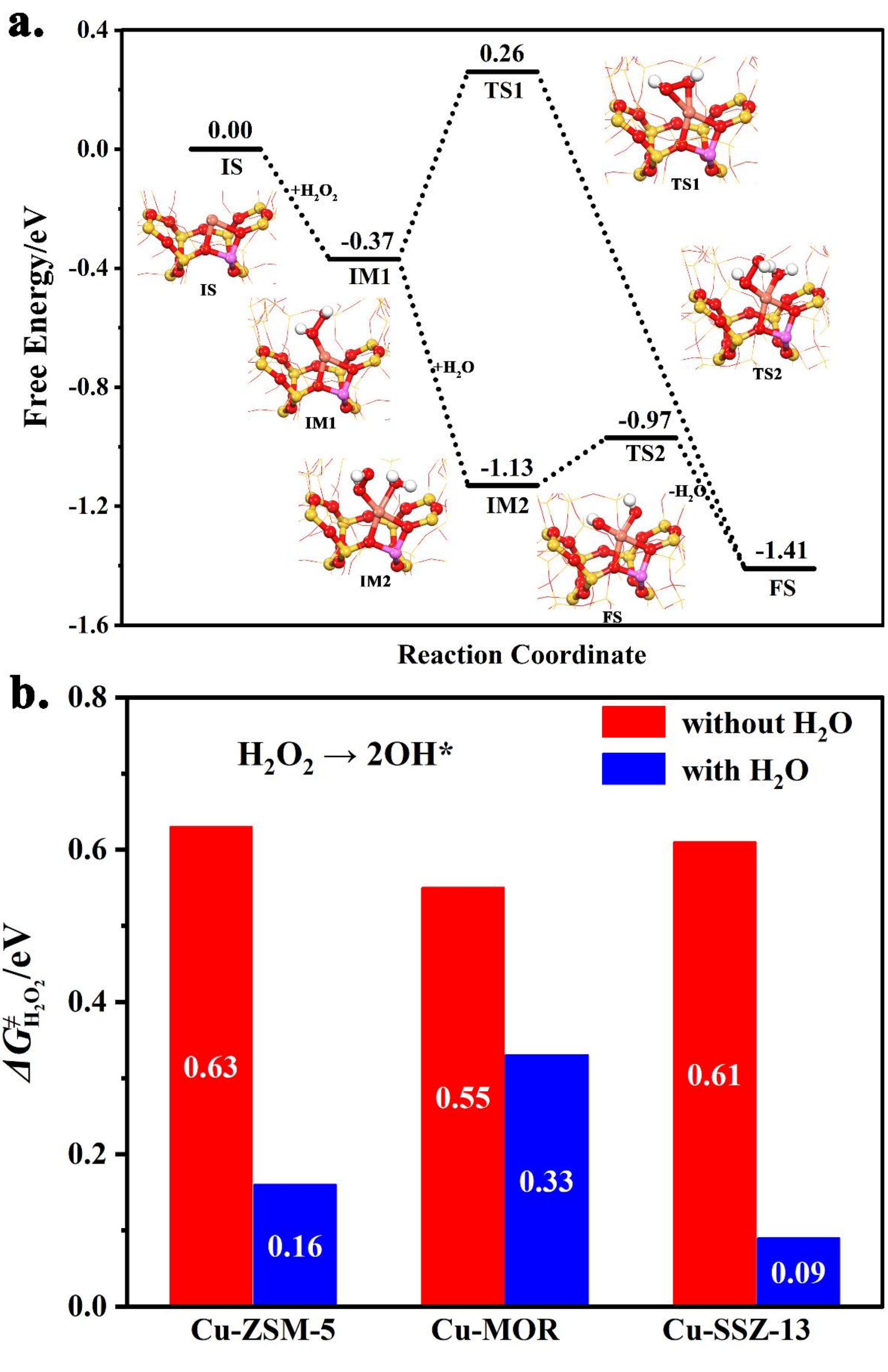

Figure 4. (a) The free energy profiles of the water-mediated and direct O-O bond activation of H_2O_2 catalyzed by $[Cu]^+$/ZSM-5 at 323 K, and **(b)** the free energies of activation for the O-O bond direct and water-mediated cleavage of H_2O_2 at Cu-ZSM-5, Cu-MOR, and Cu-SSZ-13.

The O_2 would be strongly chemisorbed at $Z[Cu]^+$ with the free energy of adsorption of -1.19 eV in Cu-ZSM-5 (**Figure 3a**). The spin charge analysis (**Figure S4a**) shows that O_2 could obtain one electron from $Z[Cu]^+$ to form $\cdot O_2^{-}*$. The O-O bond of O_2 is thereby strengthened to 1.316 Å, implying the formation of superoxide as well[77]. It is formidable for O_2 to capture more electrons to boost O-O bond activation to generate $O_2^{2-}*$ or assist the O-O bond breaking towards the generation of $O^{2-}*$. It is also similar in Cu-MOR and Cu-SSZ-13. It should be attributed to the higher intrinsic O-O bond of O_2 (498 kJ/mol) compared with hydrogen peroxide (210 kJ/mol)[78] and the valence limit from Cu cation. Hence, only the O-O bond of H_2O_2 could be cleaved at $Z[Cu]^+$.

3.2.2 C-H bond activation

We further investigated the C-H bond activation of methane. As aforementioned, $Z[Cu(OH)_2]^+$ could readily be formed in all these copper-exchanged zeolites using H_2O_2 as the oxidant. The first C-H bond of methane could be broken at $Z[Cu(OH)_2]^+$ through a radical-like mechanism[79, 80] in which only the hydrogen fragment of methane is captured by the OH at $Z[Cu(OH)_2]^+$, while the methyl forms a constrained radical in the micropore. Moreover, the radical-like mechanism could be demonstrated by the finding of the $\cdot CH_3$.[81-84] Among these copper-exchange zeolites, the lowest free energy barrier of the C-H bond activation is 0.75 eV in Cu-ZSM-5 (**Figure 3b**). Hence, the $Z[Cu(OH)_2]^+$ is likely to activate methane at a lower temperature. The further spin charge analysis indicates that the OH* at $Z[Cu(OH)_2]^+$ exhibits the radical-like characteristics (**Figure S4b**). The generation of ·OH* could easily abstract hydrogen from methane, which accounts for the lower free energy barrier of the C-H bond breaking.

On the contrary, methane activation is rather intractable at $Z[CuO_2]^+$ site. The free energy barriers in these copper-exchange zeolites are all beyond 1.52 eV (**Figure 3b**), indicating that the superoxide $\cdot O_2^{-}$* in the copper-exchange zeolites is unable to activate methane at a lower temperature.

Hence, we could find that the facile O-O bond breaking of H_2O_2 at mono-copper sites readily enables the production of surface reactive ·OH*, thereby triggering the mild C-H bond activation at a lower temperature. Consequently, hydrogen peroxide utilization could significantly promote methane activation at a lower temperature.

3.3 Methane direct conversion towards methanol

3.3.1 Methane oxidation

Based on the lowest barrier of the C-H bond activation, we further explored the complete catalytic cycle of DMTM using H_2O_2 in Cu-ZSM-5.

Since the activation of methane proceeds through a radical-like mechanism, the weakly constraint $\cdot CH_3$ in the 10-membered ring and $Z[CuOH(H_2O)]^+$ are produced followed by the facile H_2O desorption (0.23 eV) to form $Z[CuOH]^+$. The reaction pathways would branch into two from $Z[CuOH]^+$. $Z[CuOH]^+$ could either capture gaseous $\cdot CH_3$ or activate another CH_4 molecule. As shown in the blue branch of **Figure 5**, the constrained $\cdot CH_3$ is energetically easy to be captured by the reactive ·OH* at

$Z[CuOH]^+$ to produce CH_3OH^* readily (-2.01 eV). After the facile desorption of methanol (0.77 eV), the $Z[Cu]^+$ site could be regenerated.

The orange pathway in **Figure 5** shows the other potential route to proceed, starting with another methane C-H bond activation. The free energy barrier for the first C-H bond breaking of methane at $Z[CuOH]^+$ is 1.14 eV, which is higher than that at $Z[Cu(OH)_2]^+$. The desorption of resulting water (0.39 eV) enables the weak chemisorption of hydrogen peroxide for the subsequent facile O-O bond activation to generate two $OH\cdot^*$, climbing over a free energy barrier of 0.27 eV. One $OH\cdot^*$ only needs to overcome a pretty low free energy barrier of 0.10 eV to couple with CH_3^* towards CH_3OH^*. Therefore, the $Z[CuOH]^+$ is regenerated after the swift desorption of methanol (-0.22 eV). As a result, DMTM could continuously recycle at $Z[CuOH]^+$. The lower free energy barriers enable both pathways to be possibly active for DMTM using hydrogen peroxide as the oxidants. Nevertheless, compared with the catalytic cycle enclosing $Z[Cu(OH)_2]^+$, the activity of that at $Z[CuOH]^+$ would be lower due to the higher C-H bond activation barrier.

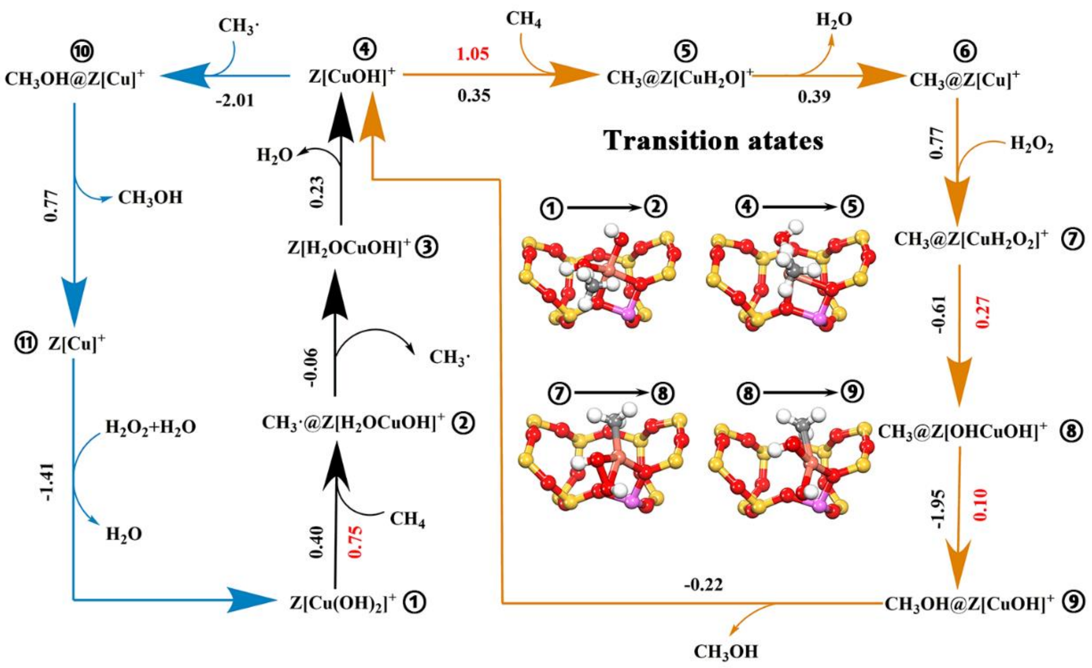

Figure 5. The reaction network of methane conversion towards methanol in Cu-ZSM-5. The reaction network starts with the black pathway. The blue and the orange arrows are the reaction cycles of regenerating Z[$Cu(OH)_2$]$^+$ and Z[CuOH]$^+$ sites, respectively. The black and red numbers respectively represent the free energy variation and the free energy of activation for each elementary step with the unit of eV. The geometry structures of some crucial transition states are also shown.

3.3.2 H_2O_2 decomposition

Although the conversion of methane is facile in mononuclear Cu zeolites, it is possible for Z[$Cu(OH)_2$]$^+$ and Z[CuOH]$^+$ sites to launch the competition process of the hydrogen peroxide decomposition as well because of the weaker H-O bond of H_2O_2 (366 kJ/mol)[78]. As depicted in **Figure 6**, the hydrogen bonding enables the H_2O_2 molecule to be stuck to Z[$Cu(OH)_2$]$^+$ (IM1) with the adsorption energy of -0.33 eV. The hydrogen atom could be readily abstracted from H_2O_2 by the ·OH* at Z[$Cu(OH)_2$]$^+$ to generate ·OOH and $Z[CuOH(H_2O)]^+$ (IM2) via a radical-like mechanism, which only needs to overcome a free energy barrier of 0.24 eV (TS1). The $Z[CuOH]^+$ (IM3) could be subsequently produced after the facile H_2O desorption from $Z[CuOH(H_2O)]^+$.

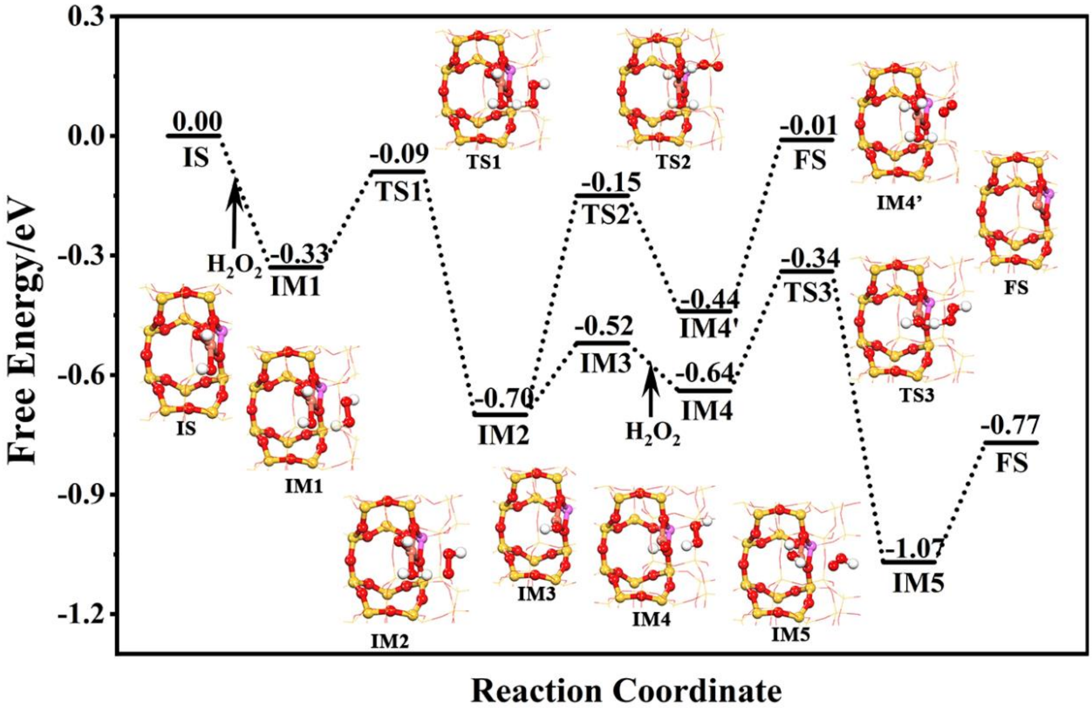

Figure 6. Gibbs free energy profiles of hydrogen peroxide oxidation at $[Cu(OH)_2]^+$/ZSM-5 site at 323 K with the geometry structures of the corresponding transition states and intermediate states.

Analogical to CH_4 activation, $Z[CuOH]^+$ could abstract a hydrogen atom from either·OOH or another H_2O_2 molecule. The free energy barrier of the oxidative dehydrogenation of ·OOH to O_2 is 0.55 eV at $Z[CuOH]^+$. The $Z[Cu]^+$ is regenerated after the facile desorption of H_2O. Another H_2O_2 activation at $Z[CuOH]^+$ is still pretty easy to generate ·OOH and H_2O*. The free energy barrier is only 0.30 eV. Similarly, the $Z[Cu]^+$ is also able to be regenerated in this pathway after the facile desorption of H_2O. Hence, H_2O_2 could be readily oxidized to O_2 or ·OOH at mono-copper sites.

3.3.3 Gaseous reactions in the micropores

As the abovementioned calculation results, the free radical $\cdot OOH$ or $\cdot CH_3$ could be generated after the hydrogen abstraction by $Z[Cu(OH)_2]^+$ or $Z[CuOH]^+$. Although these radicals could be effortlessly captured by the mono-copper active sites, they are likely to swiftly diffuse away from the active sites and proceed with the gaseous reactions in the micropores as well. We further explored the possible gaseous reactions constrained in the micropores of ZSM-5. The energetic information of the possible elementary steps is summarized in **Table 1** and **Table S1**.

It could be found from **Table 1** that the association of two radicals is considerably exothermic. Morevoer, the free energies of activation are lower, indicating that the radicals would swiftly annihilate once two radicals encounter. The concentration of radicals would therefore determine the probabilities that the reactions occur. Due to the low methane conversion rate (~1%), $\cdot OOH$ collision is the most likely bimolecular reaction. The $\cdot OOH$ is also possible to react with $\cdot CH_3$ to generate methyl peroxide (CH_3OOH).[85] It is consistent with the results from Hutchings and his colleagues that CH_3OOH could be generated during the reaction.[86] It is conceptually possible for $\cdot CH_3$ bimolecular collision to produce C_2H_6. However, the low concentration of $\cdot CH_3$ would almost inhibit this reaction.

$\cdot OOH$ or $\cdot CH_3$ could also trigger a series of chain reactions after capturing hydrogen from CH_4 or H_2O. However, it is significantly endothermic for $\cdot OOH$ to abstract the hydrogen atom from CH_4 or H_2O, as shown in **Table 1**. The resulting high energy barriers would make these reactions formidable, let alone the hydrogen abstract by $\cdot CH_3$.

Interestingly, the weaker O-O bond of H_2O_2 enables $\cdot CH_3$ to readily abstract OH from H_2O_2 to directly produce CH_3OH after overcoming a facile free energy barrier in the micropores of ZSM-5, releasing the energy of 2.00 eV. It indicates that once the first C-H bond breaking, methane would be readily converted to methanol in the presence of H_2O_2. The byproduct of reactive $\cdot OH$ could further readily abstract hydrogen from $\cdot OOH$ or H_2O_2 to produce O_2 finally. Nevertheless, it is less active than the surface $Z[Cu(OH)_2]^+$ to capture hydrogen from CH_4. Hence, O_2, CH_3OOH, and CH_3OH are possible main products from the gaseous reactions in the constrained micropores.

Table 1: The standard free energy of activation and the free energy change of each key elementary step triggered by $\cdot OOH$ and $\cdot CH_3$ in the micropores of ZSM-5 solution at 323 K.

Elementary steps	$\Delta G^{\neq}$ **(eV)**	ΔG **(eV)**
$2\cdot OOH \rightarrow H_2O_2 + O_2$	**0.48**	**-2.11**
$\cdot CH_3 + \cdot OOH \rightarrow CH_3OOH$	**0.33**	**-2.13**
$2\cdot CH_3 \rightarrow C_2H_6$	**0.41**	**-1.88**
$H_2O + \cdot OOH \rightarrow H_2O_2 + \cdot OH$	**1.62**	**1.29**
$CH_4 + \cdot OOH \rightarrow \cdot CH_3 + H_2O_2$	**1.42**	**0.75**
$\cdot CH_3 + H_2O_2 \rightarrow CH_3OH + \cdot OH$	**0.68**	**-2.15**
$CH_4 + \cdot OH \rightarrow \cdot CH_3 + H_2O$	**0.96**	**-0.68**
$\cdot OOH + \cdot OH \rightarrow H_2O + O_2$	**0.47**	**-3.39**

$H_2O_2 + \cdot OH \rightarrow H_2O + OOH$	**0.33**	**-1.29**

3.4 Competition among methane, methanol and hydrogen peroxide oxidation

Although methane could be intrinsically activated at active sites $Z[Cu(OH)_2]^+$ and $Z[CuOH]^+$, regarding the limited number of active sites, the competition among methane, methanol, and hydrogen peroxide oxidation must exist. Importantly, the selectivity depends on the competition of C-H bond activation between methane and methanol. The conversion of methane and the consumption of hydrogen peroxide are associated with the O-H bond activation of H_2O_2 and the C-H bond activation of CH_4. Hence, we computationally compared the free energy barriers of these bond activation, analyzed the different components contribution, and understood the resultant kinetic influence.

3.4.1 Oxidative dehydrogenation

The enthalpy, entropy, solvation, and concentration/partial pressure would have a combined effect on the priority of the bond activation. The cumulative bar graphs at **Figure 7** have illustrated their respective contributions for the first C-H bond breakings of methane and methanol and the first O-H bond breaking for H_2O_2 at the $Z[Cu(OH)_2]^+$ and the $Z[CuOH]^+$ sites of ZSM-5.

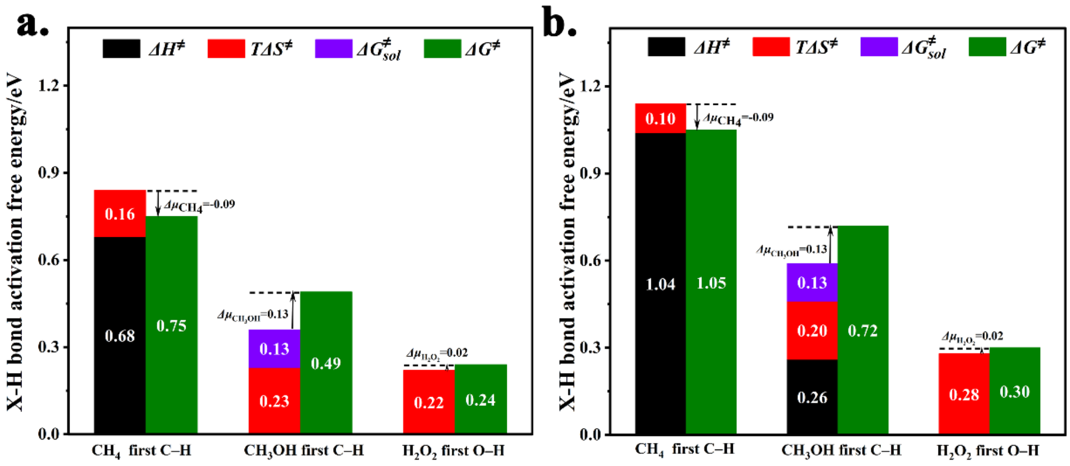

Figure 7. The cumulative bar graph for the activation free energies ***ΔG≠*** of the first C-H bond breaking of methane and methanol and the first O-H bond breaking of hydrogen peroxide at **(a)** $[Cu(OH)_2]^+$/ZSM-5 site, and **(b)** $[CuOH]^+$/ZSM-5 site. For each activation free energy, ***ΔH≠***, ***TΔS≠***, ***ΔG≠sol*** represent the contribution of enthalpy, entropy, and free energy of solvation to the free energy barrier. ***ΔG≠sol*** is calculated with reference to 1 mol/L CH_3OH solution, which corresponds to a gaseous CH_3OH partial pressure of 0.01 bar. ***Δμ*** corresponds to the influence of pressure and concentration on the free energy barrier at 323 K:30 bar CH_4,100 μmol CH_3OH/10 mL H_2O,0.51 M H_2O_2.

First, the enthalpy contribution plays a leading role in oxidative dehydrogenation. Notably, the free energy of activation $\Delta G^{\neq}$ for methane dehydrogenation is higher than those of methanol and hydrogen peroxide. It indicates that methane is the most difficult to be activated among these three molecules at these two sites. It is mainly owing to the intrinsic bond strengths of the molecules. Notably, the C-H bond strength of methane (439 kJ/mol) is greater than that of methanol (402 kJ/mol), let alone the O-H bond of H_2O_2 (366 kJ/mol). The first O-H bond activation of hydrogen peroxide even has almost zero enthalpy changes at the two sites. What's more, the hydrogen atom abstract from these molecules all occur via the radical-like mechanism at more active $Z[Cu(OH)_2]^+$, i.e., the TSs are all stabilized only by the O-H bond between OH* at $Z[Cu(OH)_2]^+$ and the reactant molecule. Thus, the intrinsic bond strength of the molecule must play the dominant role in the preferential bond activation.

Second, the entropic effect has an inverse trend against the enthalpy effect, which possibly narrows down the gap of the bond activation. Compared with methanol and hydrogen peroxide, the smaller entropy of methane results in a lower entropy loss during its activation. Thus, the entropic effect would promote the methane conversion and its selectivity for DMTM. Nonetheless, the entropic advantage of methane is trivial in the confined micropores at a low temperature.

Last but not least, the activity and the selectivity would be affected by the chemical potential variation due to the concentration/partial pressure of these molecules. The high partial pressure of methane would boost the probability of the C-H bond activation, promoting both activity and selectivity towards methanol. The resultant low concentration of methanol due to the low conversion of methane would limit the deep oxidation of methanol.

Hence, on the one hand, the generation of active sites of $[CuOH]^+$ and $[Cu(OH)_2]^+$ relies on hydrogen peroxide. On the other hand, the active sites would preferentially catalyze the self-decomposition of hydrogen peroxide. Accordingly, the oxidation of hydrogen peroxide would suppress the methane activation and its deep oxidation.

3.4.2 Kinetic analysis

We further understand the impact of the active sites and the oxidant hydrogen peroxide on the activity and selectivity for methane partial oxidation based on kinetic analysis.

We also employed the simplified kinetic model of a simple two-step mechanism proposed by Latimer et al. to simulate the limitation between selectivity and activity of DMTM. Except for the rate-determining and selectivity-determining first C-H bond cleavages of methane and methanol, all the other steps were assumed to reach the quasi-equilibrium.

$$\mathrm{CH_4} \rightarrow \mathrm{CH_3OH} \rightarrow \mathrm{CO_2} \tag{5}$$

where the desired product methanol is thereby a transition intermediate. The selectivity towards methanol ($S_{\mathrm{CH_3OH}}$) can be expressed as a function of methane conversion rate (X) and the difference of the free energies of activation ($\Delta G_1^{\neq}$) between the first C-H bond breaking of methane ($\Delta G_{\mathrm{CH_4}}^{\neq}$) and methanol ($\Delta G_{\mathrm{CH_3OH}}^{\neq}$) as follows:

$$S_{\mathrm{CH_3OH}} = \frac{1-X-(1-X)^{e^{\Delta G_1^{\neq}/RT}}}{X\cdot e^{\Delta G_1^{\neq}/RT}-1} \tag{6}$$

$$\text{where } \Delta G_1^{\neq} = \Delta G_{\mathrm{CH_4}}^{\neq} - \Delta G_{\mathrm{CH_3OH}}^{\neq} \tag{7}$$

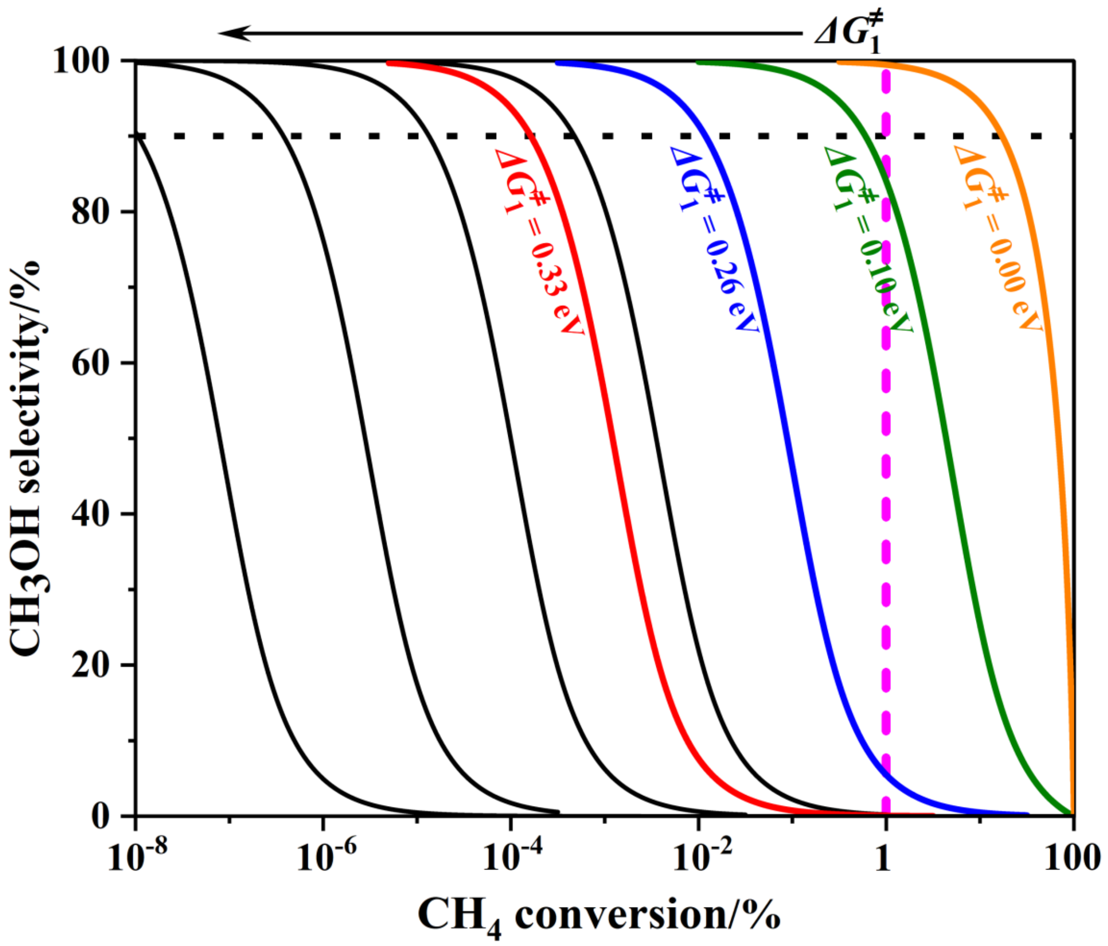

Figure 8. The relationship between the conversion rate and methanol selectivity at different times was investigated. The red line corresponds to the real situation of the $Z[CuOH]^+$ site; The blue line corresponds to the real situation of the $Z[Cu(OH)_2]^+$ site. Reaction conditions: 28 mg catalysts dispersed in 10 ml of 0.51 M H_2O_2 aqueous solution, 30 bar CH_4 for 30 min.

Since the C-H bond activations all occur via the radical-like mechanism at $Z[Cu(OH)_2]^+$ in Cu-exchanged zeolites, methanol is always easier to be activated, i.e., $\Delta G_1^{\neq} > 0$, the selectivity of methanol and the activity of methane oxidation is always mutually inhibited. The smaller $\Delta G_1^{\neq}$ is significantly beneficial to DMTM. Among the investigated zeolites, the minimum gaps of the free energies of activation between methane and methanol dehydrogenation are achieved at the $Z[Cu(OH)_2]^+$ and the

$Z[CuOH]^+$ sites in ZSM-5, respectively 0.26 eV and 0.33 eV. As seen from **Figure 8**, the conversion rate of methane is rather low at these sites when the desired selectivity towards methanol is higher than 90%. If the conversion rate of methane is expected to arrive at 10% with a selectivity of 90% towards methanol, then $\Delta G_1^{\neq}$ must be lower than 0.10 eV to achieve the same selectivity. Hence, the high selectivity towards methanol with high conversion must face the tremendous challenge of using H_2O_2 as the oxidant. On the other hand, if the 10% conversion is obtained in 24 h, then it indicates that the corresponding turnover frequency (TOF) is 2340 h^{-1}. This TOF is still significantly higher than the previously reported results.[34, 48, 49, 75, 87, 88] Despite the existence of the bottleneck due to the activity-selectivity trade-off, it is still promising to improve DMTM catalysts using H_2O_2 as the oxidant in the future.

In addition, the active $Z[Cu(OH)_2]^+$ and $Z[CuOH]^+$ sites are energetically more favorable to activate hydrogen peroxide. Competition exists between the conversion of methane and hydrogen peroxide. The ratio of reaction rates between methane and hydrogen peroxide conversion could be expressed as follows:

$$\frac{k_{\mathrm{CH_4}}}{k_{\mathrm{H_2O_2}}} = \mathrm{e}^{-(\Delta G_2^{\neq})/RT} \tag{9}$$

$$\Delta G_2^{\neq} = \Delta G_{\mathrm{CH_4}}^{\neq} - \Delta G_{\mathrm{H_2O_2}}^{\neq} \tag{10}$$

where $\Delta G_2^{\neq}$ is the difference of the free energies of activation between the first methane C-H bond cleavage and the second hydrogen peroxide O-H bond cleavage. These two steps are the rate-determining steps for methane and hydrogen peroxide oxidation, respectively. As displayed in **Figure 9**, the highest methane conversion is obtained at $[Cu(OH)_2]^+$/ZSM-5 among the investigated mono-copper active sites. However, the self-decomposition of hydrogen peroxide is still overwhelming. It is consistent with the experimental observation of Yashnik et al..[89] Nevertheless, since the Z[Cu(OH)$_2$]$^+$ and Z[CuOH]$^+$ sites would mainly catalyze the self-decomposition of hydrogen peroxide, the rate of methanol oxidation would be significantly suppressed, preventing methane from the deep oxidation. Hence, the reported high selectivity toward methanol for DMTM using hydrogen peroxide at copper-zeolites may be related to the low methane conversion.

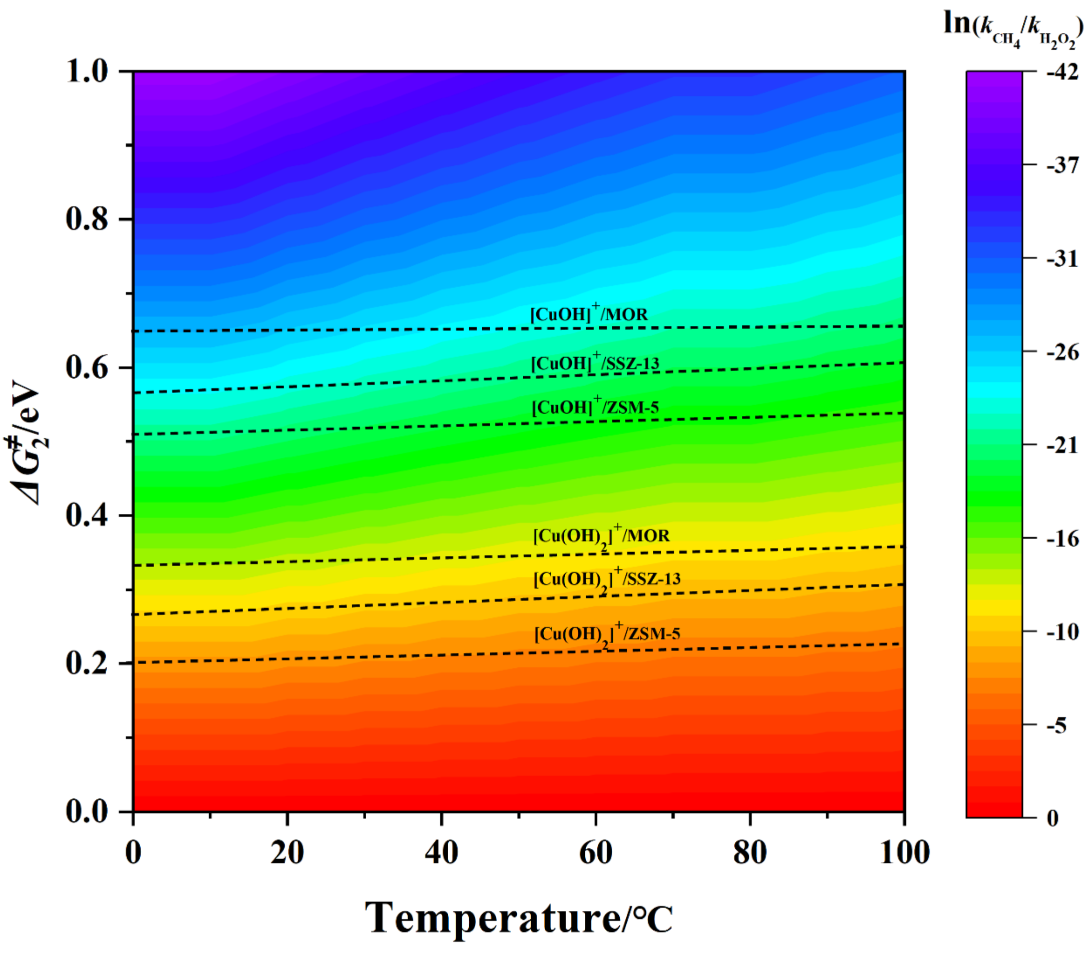

Figure 9. The ratio of the conversion rate of methane and hydrogen peroxide oxidation against the difference of the free energy of activation between the first C-H bond breaking of methane and the second O-H bond breaking of hydrogen peroxide and temperature.

It might be a common problem for DMTM using hydrogen peroxide as the oxidant that the active site prefers catalyzing self-decomposition of hydrogen peroxide. Pidko and his colleagues also found that hydrogen peroxide is not suitable for methane oxidation catalyzed by iron-based materials.[85, 90] Although Xiao's group reported that the addition of Brönsted acid could inhibit the self-decomposition of hydrogen peroxide,[91] it might also hinder the C-H bond breaking. The inhibited self-decomposition mainly results from Le Chatelier's principle whereby the higher concentration of Brönsted acid prevents the equilibrium from offsetting towards the dehydrogenation. Likewise, it could obstruct the C-H bond breaking as well. Still, the self-decomposition of hydrogen peroxide would be superior to methane conversion. Hence, the excessive consumption of hydrogen peroxide is inevitable for DMTM when using hydrogen peroxide as the oxidant. Moreover, the common problem of the trade-off between selectivity and activity still exists for DMTM.

4. Conclusion

Our theoretical calculation unravels that the O-O bond could be readily broken to form surface reactive hydroxyl through a water-mediated mechanism in mononuclear copper zeolites using hydrogen peroxide as the oxidant to form reactive $Z[Cu(OH)_2]^+$. It enables the mild C-H bond activation of methane at a low temperature. On the contrary, the O-O bond of dioxygen is formidable to be scissored to produce reactive surface oxygen species at mono-copper sites, resulting in the formidable C-H bond activation of methane at the low temperature. Hydrogen peroxide exhibits a higher reactivity for methane activation compared with molecular oxygen.

Although methane and hydrogen peroxide can easily react to form methanol at the active site, we find that the $Z[Cu(OH)_2]^+$ could preferentially catalyze the deep oxidation of methanol and the self-decomposition of hydrogen peroxide. The C-H bond and O-H bond activation occur via the radical-like mechanism at $Z[Cu(OH)_2]^+$. The further kinetic analysis discloses that the radical-like mechanism would result in the inevitable trade-off between the selectivity and activity for DMTM using hydrogen peroxide. Moreover, the self-decomposition of hydrogen peroxide would be dominant. Hence, the high selectivity of methanol is achieved for DMTM using hydrogen peroxide at the cost of the low conversion of methane and the waste of hydrogen peroxide. Nevertheless, the kinetic analysis unravels that it is still promising to improve DMTM catalysts using hydrogen peroxide to achieve the higher TOF of DMTM despite the bottleneck of the activity-selectivity trade-off.

Supporting Information

The phase diagram of $\mathrm{Cu}_x\mathrm{O}_y\mathrm{H}_z$ complexes in zeolite, the optimized structures of mono-copper species in Cu-MOR, the optimized structures of mono-copper species in Cu-SSZ-13, spin charge densities of $[CuO_2]^+$/ZSM-5 and $[Cu(OH)_2]^+$/ZSM-5, the reaction mechanisms of H_2O_2 activation in $[Cu]^+$/MOR and $[Cu]^+$/SSZ-13, and the possible gaseous radical elementary steps in the micropores of ZSM-5

Conflicts of Interest

There are no conflicts to declare.

Acknowledgements

This work was financially supported by National Key Research and Development Program of China (2018YFA0208600), National Natural Science Foundation of China (91845111, 22022302, 92045303), Shanghai Municipal Science and Technology Major Project (2018SHZDZX03), the Program of Introducing Talents of Discipline to Universities (B16017) and the Fundamental Research Funds for the Central Universities(JKVJ1211040).

References

1. Global, B.; Worldwide, B., BP Energy Outlook 2030. *London, UK* **2011**.
2. Olah, G. A., Jenseits von öl und Gas: die Methanolwirtschaft. *Angewandte Chemie* **2005,** *117* (18), 2692-2696.
3. Olah, G. A., Methanol is produced nearly exclusively from synthesis gas (CO-f-H2). *Angew. Chem. Int. Ed* **2005,** *44*, 2636-2639.
4. Elvidge, C. D.; Zhizhin, M.; Baugh, K.; Hsu, F.-C.; Ghosh, T., Methods for global survey of natural gas flaring from visible infrared imaging radiometer suite data. *Energies* **2016,** *9* (1), 14.
5. Ravi, M.; Ranocchiari, M.; van Bokhoven, J. A., The direct catalytic oxidation of methane to methanol—a critical assessment. *Angewandte Chemie International Edition* **2017,** *56* (52), 16464-16483.
6. Parkyns, N.; Warburton, C.; Wilson, J., Natural gas conversion to liquid fuels and chemicals: Where does it stand? *Catalysis today* **1993,** *18* (4), 385-442.
7. Hammond, C.; Conrad, S.; Hermans, I., Oxidative methane upgrading. *ChemSusChem* **2012,** *5* (9), 1668-1686.
8. Roudesly, F.; Oble, J.; Poli, G., Metal-catalyzed CH activation/functionalization: The fundamentals. *Journal of Molecular Catalysis A: Chemical* **2017,** *426*, 275-296.
9. Olivos-Suarez, A. I.; Szécsényi, A. g.; Hensen, E. J.; Ruiz-Martinez, J.; Pidko, E. A.; Gascon, J., Strategies for the direct catalytic valorization of methane using heterogeneous catalysis: challenges and opportunities. *Acs Catalysis* **2016,** *6* (5), 2965-2981.
10. Pannov, G.; Sobolev, V.; Kharitonov, A., The role of iron in N2O decomposition on ZSM-5 zeolite and reactivity of the surface oxygen formed. *Journal of molecular catalysis* **1990,** *61* (1), 85-97.
11. Rostrup-Nielsen, J. R.; Sehested, J.; Nørskov, J. K., Hydrogen and synthesis gas by steam-and C02 reforming. **2002,** *47*, 65-139.
12. Bergman, R. G., C–H activation. *Nature* **2007,** *446* (7134), 391-393.
13. Starokon, E. V.; Parfenov, M. V.; Pirutko, L. V.; Abornev, S. I.; Panov, G. I., Room-temperature oxidation of methane by α-oxygen and extraction of products from the FeZSM-5 surface. *The Journal of Physical Chemistry C* **2011,** *115* (5), 2155-2161.

14. Hammond, C.; Dimitratos, N.; Lopez-Sanchez, J. A.; Jenkins, R. L.; Whiting, G.; Kondrat, S. A.; Ab Rahim, M. H.; Forde, M. M.; Thetford, A.; Hagen, H., Aqueous-phase methane oxidation over Fe-MFI zeolites; promotion through isomorphous framework substitution. *ACS Catalysis* **2013,** *3* (8), 1835-1844.
15. Müller, K.; Fabisch, F.; Arlt, W., Energy transport and storage using methanol as a carrier. *Green* **2014,** *4* (1-6), 19-25.
16. Schwach, P.; Pan, X.; Bao, X., Direct conversion of methane to value-added chemicals over heterogeneous catalysts: challenges and prospects. *Chemical reviews* **2017,** *117* (13), 8497-8520.
17. Xie, S.; Lin, S.; Zhang, Q.; Tian, Z.; Wang, Y., Selective electrocatalytic conversion of methane to fuels and chemicals. *Journal of energy chemistry* **2018,** *27* (6), 1629-1636.
18. Banerjee, R.; Proshlyakov, Y.; Lipscomb, J. D.; Proshlyakov, D. A., Structure of the key species in the enzymatic oxidation of methane to methanol. *Nature* **2015,** *518* (7539), 431-434.
19. Sharma, R.; Poelman, H.; Marin, G. B.; Galvita, V. V., Approaches for Selective Oxidation of Methane to Methanol. *Catalysts* **2020,** *10* (2).
20. Rosenzweig, A. C.; Frederick, C. A.; Lippard, S. J., Crystal structure of a bacterial non-haem iron hydroxylase that catalyses the biological oxidation of methane. *Nature* **1993,** *366* (6455), 537-543.
21. Bordeaux, M.; Galarneau, A.; Drone, J., Catalytic, mild, and selective oxyfunctionalization of linear alkanes: current challenges. *Angewandte Chemie International Edition* **2012,** *51* (43), 10712-10723.
22. Sirajuddin, S.; Rosenzweig, A. C., Enzymatic oxidation of methane. *Biochemistry* **2015,** *54* (14), 2283-2294.
23. Smeets, P. J.; Groothaert, M. H.; Schoonheydt, R. A., Cu based zeolites: A UV–vis study of the active site in the selective methane oxidation at low temperatures. *Catalysis today* **2005,** *110* (3-4), 303-309.
24. Alayon, E. M. C.; Nachtegaal, M.; Bodi, A.; van Bokhoven, J. A., Reaction conditions of methane-to-methanol conversion affect the structure of active copper sites. *ACS Catalysis* **2014,** *4* (1), 16-22.
25. Brezicki, G.; Zheng, J.; Paolucci, C.; Schlögl, R.; Davis, R. J., Effect of the Co-cation on Cu Speciation in Cu-Exchanged Mordenite and ZSM-5 Catalysts for the Oxidation of Methane to Methanol. *ACS Catalysis* **2021,** *11*, 4973-4987.
26. Groothaert, M. H.; Smeets, P. J.; Sels, B. F.; Jacobs, P. A.; Schoonheydt, R. A., Selective oxidation of methane by the bis (μ-oxo) dicopper core stabilized on ZSM-5 and mordenite zeolites. *Journal of the American Chemical Society* **2005,** *127* (5), 1394-1395.
27. Groothaert, M. H.; van Bokhoven, J. A.; Battiston, A. A.; Weckhuysen, B. M.; Schoonheydt, R. A., Bis (μ-oxo) dicopper in Cu-ZSM-5 and its role in the decomposition of NO: a combined in situ XAFS, UV− Vis− Near-IR, and kinetic study. *Journal of the American Chemical Society* **2003,** *125* (25), 7629-7640.
28. Yumura, T.; Hirose, Y.; Wakasugi, T.; Kuroda, Y.; Kobayashi, H., Roles of water molecules in modulating the reactivity of dioxygen-bound Cu-ZSM-5 toward methane: a theoretical prediction. *ACS Catalysis* **2016,** *6* (4), 2487-2495.
29. Narsimhan, K.; Iyoki, K.; Dinh, K.; Román-Leshkov, Y., Catalytic oxidation of methane into methanol over copper-exchanged zeolites with oxygen at low temperature. *ACS central science* **2016,** *2* (6), 424-429.
30. Grundner, S.; Markovits, M. A.; Li, G.; Tromp, M.; Pidko, E. A.; Hensen, E. J.; Jentys,

A.; Sanchez-Sanchez, M.; Lercher, J. A., Single-site trinuclear copper oxygen clusters in mordenite for selective conversion of methane to methanol. *Nature communications* **2015,** *6* (1), 1-9.

31. Sushkevich, V. L.; Palagin, D.; Ranocchiari, M.; van Bokhoven, J. A., Selective anaerobic oxidation of methane enables direct synthesis of methanol. *Science* **2017,** *356* (6337), 523-527.

32. Pappas, D. K.; Borfecchia, E.; Dyballa, M.; Pankin, I. A.; Lomachenko, K. A.; Martini, A.; Signorile, M.; Teketel, S.; Arstad, B.; Berlier, G., Methane to methanol: structure–activity relationships for Cu-CHA. *Journal of the American Chemical Society* **2017,** *139* (42), 14961-14975.

33. Pappas, D. K.; Martini, A.; Dyballa, M.; Kvande, K.; Teketel, S.; Lomachenko, K. A.; Baran, R.; Glatzel, P.; Arstad, B.; Berlier, G., The nuclearity of the active site for methane to methanol conversion in Cu-mordenite: a quantitative assessment. *Journal of the American Chemical Society* **2018,** *140* (45), 15270-15278.

34. Sun, L.; Wang, Y.; Wang, C.; Xie, Z.; Guan, N.; Li, L., Water-involved methane-selective catalytic oxidation by dioxygen over copper zeolites. *Chem* **2021,** *7* (6), 1557-1568.

35. Beznis, N. V.; Weckhuysen, B. M.; Bitter, J. H., Cu-ZSM-5 zeolites for the formation of methanol from methane and oxygen: Probing the active sites and spectator species. *Catalysis letters* **2010,** *138* (1), 14-22.

36. Vanelderen, P.; Vancauwenbergh, J.; Sels, B. F.; Schoonheydt, R. A., Coordination chemistry and reactivity of copper in zeolites. *Coordination Chemistry Reviews* **2013,** *257* (2), 483-494.

37. Spoto, G.; Gribov, E.; Bordiga, S.; Lamberti, C.; Ricchiardi, G.; Scarano, D.; Zecchina, A., Cu+(H 2) and Na+(H 2) adducts in exchanged ZSM-5 zeolites. *Chemical communications* **2004,** (23), 2768-2769.

38. Vanelderen, P.; Snyder, B. E.; Tsai, M.-L.; Hadt, R. G.; Vancauwenbergh, J.; Coussens, O.; Schoonheydt, R. A.; Sels, B. F.; Solomon, E. I., Spectroscopic definition of the copper active sites in mordenite: selective methane oxidation. *Journal of the American Chemical Society* **2015,** *137* (19), 6383-6392.

39. Newton, M. A.; Knorpp, A. J.; Pinar, A. B.; Sushkevich, V. L.; Palagin, D.; van Bokhoven, J. A., On the mechanism underlying the direct conversion of methane to methanol by copper hosted in zeolites; braiding Cu K-Edge XANES and reactivity Studies. *Journal of the American Chemical Society* **2018,** *140* (32), 10090-10093.

40. Park, M. B.; Ahn, S. H.; Mansouri, A.; Ranocchiari, M.; van Bokhoven, J. A., Comparative study of diverse copper zeolites for the conversion of methane into methanol. *ChemCatChem* **2017,** *9* (19), 3705-3713.

41. Sushkevich, V. L.; Verel, R.; van Bokhoven, J. A., Pathways of Methane Transformation over Copper-Exchanged Mordenite as Revealed by In Situ NMR and IR Spectroscopy. *Angew Chem Int Ed Engl* **2020,** *59* (2), 910-918.

42. Meyet, J.; Searles, K.; Newton, M. A.; Worle, M.; van Bavel, A. P.; Horton, A. D.; van Bokhoven, J. A.; Coperet, C., Monomeric Copper(II) Sites Supported on Alumina Selectively Convert Methane to Methanol. *Angew Chem Int Ed Engl* **2019,** *58* (29), 9841-9845.

43. Kulkarni, A. R.; Zhao, Z.-J.; Siahrostami, S.; Nørskov, J. K.; Studt, F., Monocopper active site for partial methane oxidation in Cu-exchanged 8MR zeolites. *ACS Catalysis* **2016,** *6* (10), 6531-6536.

44. Yashnik, S. A.; Ismagilov, Z. R.; Anufrienko, V. F., Catalytic properties and electronic structure of copper ions in Cu-ZSM-5. *Catalysis today* **2005,** *110* (3-4), 310-322.

45. Kolganov, A. A.; Gabrienko, A. A.; Yashnik, S. A.; Pidko, E. A.; Stepanov, A. G., Nature of the surface intermediates formed from methane on Cu-ZSM-5 zeolite: A combined solid-state nuclear

magnetic resonance and density functional theory study. *The Journal of Physical Chemistry C* **2020,** *124* (11), 6242-6252.

46. Meyet, J.; Searles, K.; Newton, M. A.; Wörle, M.; van Bavel, A. P.; Horton, A. D.; van Bokhoven, J. A.; Copéret, C., Monomeric copper (II) sites supported on alumina selectively convert methane to methanol. *Angewandte Chemie* **2019,** *131* (29), 9946-9950.

47. Yan, Y.; Chen, C.; Zou, S.; Liu, J.; Xiao, L.; Fan, J., High H2O2 utilization promotes selective oxidation of methane to methanol at low temperature. *Frontiers in chemistry* **2020,** *8*, 252.

48. Armstrong, R. D.; Peneau, V.; Ritterskamp, N.; Kiely, C. J.; Taylor, S. H.; Hutchings, G. J., The Role of Copper Speciation in the Low Temperature Oxidative Upgrading of Short Chain Alkanes over Cu/ZSM-5 Catalysts. *ChemPhysChem* **2018,** *19* (4), 469-478.

49. Tang, X.; Wang, L.; Yang, B.; Fei, C.; Yao, T.; Liu, W.; Lou, Y.; Dai, Q.; Cai, Y.; Cao, X.-M., Direct oxidation of methane to oxygenates on supported single Cu atom catalyst. *Applied Catalysis B: Environmental* **2021,** *285*, 119827.

50. Shulpin, G.; Nizova, G., Formation of alkyl peroxides in oxidation of alkanes by H 2 O 2 catalyzed by transition metal complexes. *Reaction Kinetics and Catalysis Letters* **1992,** *48* (1), 333-338.

51. Pestovsky, O.; Stoian, S.; Bominaar, E. L.; Shan, X.; Münck, E.; Que Jr, L.; Bakac, A., Aqueous FeIV□O: Spectroscopic Identification and Oxo-Group Exchange. *Angewandte Chemie* **2005,** *117* (42), 7031-7034.

52. Kresse, G.; Furthmüller, J., Efficiency of ab-initio total energy calculations for metals and semiconductors using a plane-wave basis set. *Computational materials science* **1996,** *6* (1), 15-50.

53. Kresse, G.; Furthmüller, J., Efficient iterative schemes for ab initio total-energy calculations using a plane-wave basis set. *Physical review B* **1996,** *54* (16), 11169.

54. Kresse, G.; Hafner, J., Ab initio molecular dynamics for liquid metals. *Physical Review B* **1993,** *47* (1), 558.

55. Kresse, G.; Hafner, J., Ab initio molecular-dynamics simulation of the liquid-metal–amorphous-semiconductor transition in germanium. *Physical Review B* **1994,** *49* (20), 14251.

56. Perdew, J. P.; Burke, K.; Ernzerhof, M., Generalized gradient approximation made simple. *Physical review letters* **1996,** *77* (18), 3865.

57. Grimme, S.; Antony, J.; Ehrlich, S.; Krieg, H., A consistent and accurate ab initio parametrization of density functional dispersion correction (DFT-D) for the 94 elements H-Pu. *The Journal of chemical physics* **2010,** *132* (15), 154104.

58. Grimme, S.; Ehrlich, S.; Goerigk, L., Effect of the damping function in dispersion corrected density functional theory. *Journal of computational chemistry* **2011,** *32* (7), 1456-1465.

59. Alavi, A.; Hu, P.; Deutsch, T.; Silvestrelli, P. L.; Hutter, J., CO oxidation on Pt (111): An ab initio density functional theory study. *Physical Review Letters* **1998,** *80* (16), 3650.

60. Frisch, M. J., Gaussian09. *http://www. gaussian. com/* **2009**.

61. Hu, W.; Shao, Z.-J.; Cao, X.-M.; Hu, P., Multi sites vs single site for catalytic combustion of methane over Co3O4 (110): A first-principles kinetic Monte Carlo study. *Chinese Journal of Catalysis* **2020,** *41* (9), 1369-1377.

62. Lou, Y.; Cai, Y.; Hu, W.; Wang, L.; Dai, Q.; Zhan, W.; Guo, Y.; Hu, P.; Cao, X.-M.; Liu, J., Identification of active area as active center for CO oxidation over single Au atom catalyst. *ACS Catalysis* **2020,** *10* (11), 6094-6101.

63. Frisch, M.; Trucks, G.; Schlegel, H.; Scuseria, G.; Robb, M.; Cheeseman, J.; Scalmani, G.; Barone, V.; Petersson, G.; Nakatsuji, H., Gaussian 16 Rev. B. 01, Wallingford, CT. **2016**.

64. Ho, J.; Klamt, A.; Coote, M. L., Comment on the correct use of continuum solvent models. *The journal of physical chemistry A* **2010,** *114* (51), 13442-13444.
65. Dauenhauer, P. J.; Abdelrahman, O. A., A universal descriptor for the entropy of adsorbed molecules in confined spaces. *ACS central science* **2018,** *4* (9), 1235-1243.
66. Jørgensen, M.; Chen, L.; Grönbeck, H., Monte Carlo potential energy sampling for molecular entropy in zeolites. *The Journal of Physical Chemistry C* **2018,** *122* (35), 20351-20357.
67. Van Koningsveld, H.; Jansen, J.; Van Bekkum, H., The monoclinic framework structure of zeolite H-ZSM-5. Comparison with the orthorhombic framework of as-synthesized ZSM-5. *Zeolites* **1990,** *10* (4), 235-242.
68. Baerlocher, C., Database of zeolite structures. *http://www. iza-structure. org/databases/* **2008**.
69. Godiksen, A.; Stappen, F. N.; Vennestrøm, P. N.; Giordanino, F.; Rasmussen, S. B.; Lundegaard, L. F.; Mossin, S., Coordination environment of copper sites in Cu-CHA zeolite investigated by electron paramagnetic resonance. *The Journal of Physical Chemistry C* **2014,** *118* (40), 23126-23138.
70. Sushkevich, V. L.; Verel, R.; van Bokhoven, J. A., Pathways of Methane Transformation over Copper-Exchanged Mordenite as Revealed by In Situ NMR and IR Spectroscopy. *Angewandte Chemie* **2020,** *132* (2), 920-928.
71. Sushkevich, V. L.; Palagin, D.; van Bokhoven, J. A., The Effect of the Active-Site Structure on the Activity of Copper Mordenite in the Aerobic and Anaerobic Conversion of Methane into Methanol. *Angewandte Chemie* **2018,** *130* (29), 9044-9048.
72. Lonsinger, S. R.; Chakraborty, A. K.; Theodorou, D. N.; Bell, A. T., The effects of local structural relaxation on aluminum siting within H-ZSM-5. *Catalysis letters* **1991,** *11* (2), 209-217.
73. Borry, R. W.; Kim, Y. H.; Huffsmith, A.; Reimer, J. A.; Iglesia, E., Structure and density of Mo and acid sites in Mo-exchanged H-ZSM5 catalysts for nonoxidative methane conversion. *The Journal of Physical Chemistry B* **1999,** *103* (28), 5787-5796.
74. Ipek, B.; Wulfers, M. J.; Kim, H.; Goltl, F.; Hermans, I.; Smith, J. P.; Booksh, K. S.; Brown, C. M.; Lobo, R. F., Formation of [Cu2O2] 2+ and [Cu2O] 2+ toward C–H bond activation in Cu-SSZ-13 and Cu-SSZ-39. *ACS Catalysis* **2017,** *7* (7), 4291-4303.
75. Brezicki, G.; Zheng, J.; Paolucci, C.; Schlögl, R.; Davis, R. J., Effect of the Co-cation on Cu Speciation in Cu-Exchanged Mordenite and ZSM-5 Catalysts for the Oxidation of Methane to Methanol. *ACS Catalysis* **2021,** *11* (9), 4973-4987.
76. Lide, D. R., *CRC handbook of chemistry and physics*. CRC press: 2004; Vol. 85.
77. Cao, X.-M.; Zhou, H.; Zhao, L.; Chen, X.; Hu, P., Screening performance of methane activation over atomically dispersed metal catalysts on defective boron nitride monolayers: A density functional theory study. *Chinese Chemical Letters* **2021,** *32* (6), 1972-1976.
78. Johnson III, R. D., NIST computational chemistry comparison and benchmark database, NIST standard reference database number 101. *Release 16a http://cccbdb. nist. gov/(accessed Mar 13, 2015)* **2013**.
79. Xu, J.; Cao, X.-M.; Hu, P., Improved Prediction for the Methane Activation Mechanism on Rutile Metal Oxides by a Machine Learning Model with Geometrical Descriptors. *The Journal of Physical Chemistry C* **2019,** *123* (47), 28802-28810.
80. Latimer, A. A.; Aljama, H.; Kakekhani, A.; Yoo, J. S.; Kulkarni, A.; Tsai, C.; Garcia-Melchor, M.; Abild-Pedersen, F.; Nørskov, J. K., Mechanistic insights into heterogeneous methane activation. *Physical Chemistry Chemical Physics* **2017,** *19* (5), 3575-3581.
81. Kulkarni, A. R.; Zhao, Z.-J.; Siahrostami, S.; Nørskov, J. K.; Studt, F., Cation-exchanged

zeolites for the selective oxidation of methane to methanol. *Catalysis Science & Technology* **2018,** *8* (1), 114-123.
82. Dinh, K. T.; Sullivan, M. M.; Serna, P.; Meyer, R. J.; Román-Leshkov, Y., Breaking the Selectivity-Conversion Limit of Partial Methane Oxidation with Tandem Heterogeneous Catalysts. *ACS Catalysis* **2021,** *11* (15), 9262-9270.
83. Yu, T.; Li, Z.; Lin, L.; Chu, S.; Su, Y.; Song, W.; Wang, A.; Weckhuysen, B. M.; Luo, W., Highly Selective Oxidation of Methane into Methanol over Cu-Promoted Monomeric Fe/ZSM-5. *ACS Catalysis* **2021,** *11*, 6684-6691.
84. Xu, R.; Liu, N.; Dai, C.; Li, Y.; Zhang, J.; Wu, B.; Yu, G.; Chen, B., H2O-Built Proton Transfer Bridge Pronouncedly Enhances Continuous Methane Oxidation to Methanol over Cu-BEA Zeolite. *Angewandte Chemie* **2021,** *133* (30), 16770-16776.
85. Szécsényi, A. g.; Li, G.; Gascon, J.; Pidko, E. A., Mechanistic complexity of methane oxidation with H2O2 by single-site Fe/ZSM-5 catalyst. *ACS catalysis* **2018,** *8* (9), 7961-7972.
86. Hammond, C.; Forde, M. M.; Ab Rahim, M. H.; Thetford, A.; He, Q.; Jenkins, R. L.; Dimitratos, N.; Lopez-Sanchez, J. A.; Dummer, N. F.; Murphy, D. M., Direct catalytic conversion of methane to methanol in an aqueous medium by using copper-promoted Fe-ZSM-5. *Angewandte Chemie* **2012,** *124* (21), 5219-5223.
87. Fang, Z.; Huang, M.; Liu, B.; Jiang, F.; Xu, Y.; Liu, X., Identifying the crucial role of water and chloride for efficient mild oxidation of methane to methanol over a [Cu2 (μ-O)] 2+-ZSM-5 catalyst. *Journal of Catalysis* **2022,** *405*, 1-14.
88. Freakley, S. J.; Dimitratos, N.; Willock, D. J.; Taylor, S. H.; Kiely, C. J.; Hutchings, G. J., Methane Oxidation to Methanol in Water. *Accounts of Chemical Research* **2021**, 5129-5133.
89. Yashnik, S. A.; Boltenkov, V. V.; Babushkin, D. E.; Taran, O. P.; Parmon, V. N., Methane Oxidation by H 2 O 2 over Different Cu-Species of Cu-ZSM-5 Catalysts. *Topics in Catalysis* **2020,** *63* (1), 203-221.
90. Szécsényi, Á.; Li, G.; Gascon, J.; Pidko, E. A., Unraveling reaction networks behind the catalytic oxidation of methane with H 2 O 2 over a mixed-metal MIL-53 (Al, Fe) MOF catalyst. *Chemical science* **2018,** *9* (33), 6765-6773.
91. Jin, Z.; Liu, Y.; Wang, L.; Wang, C.; Wu, Z.; Zhu, Q.; Wang, L.; Xiao, F.-S., Direct Synthesis of Pure Aqueous H2O2 Solution within Aluminosilicate Zeolite Crystals. *ACS Catalysis* **2021,** *11* (4), 1946-1951.